Liquid Crystalline Octahedral Iron(III) Complexes with 1,4,7-Tris[3,4-bis-(decyloxy)benzyl]-1,4,7-triazacyclononane: Thermal Characterization and Mössbauer Investigations of Bridging and Redox Behavior

G. Henning Walf, Rüdiger. Benda, F. Jochen Litterst,* Uwe Stebani, Steven Schmidt, and Günter Lattermann*

Abstract: The complexation of iron(III) chloride with 1,4,7-tris[3,4-bis(decyloxy)-benzyl]-1,4,7-triazacyclononane leads to a liquid crystalline product, which forms a second mesophase after thermal treatment at around 70 °C above the first clearing temperature. Polarizing microscopy, DSC, and UV observations reveal a transformation, which was further investigated by Mössbauer spectroscopy. In different temperature ranges, various octahedral, binuclear iron(III) complexes are present along with a monomeric species. In the presence of water and oxygen, the iron(III) center participates in a redox equilibrium.

Keywords: bridging ligands · iron · liquid crystals · Moessbauer spectroscopy · redox chemistry

Introduction

The possibility of combining the properties of liquid crystals and metal complexes has led to intensive research on metallomesogens.[1–5] The great majority of them exhibit linear or square planar geometry at the metal center. However, because of the dependence of the physical properties (e.g. magnetism, color) on the geometry of the related ligand field, it is highly desirable to vary the geometry of the complex. In 1992 an octahedral liquid crystalline nickel(II) complex was reported.[6] Details of a further series of octahedral metal complexes, containing various ligands and forming smectic or columnar mesophases, have been published recently.[7–14] In the past, a limited number of low molecular[15–25,8] and polymeric[26–28,21] liquid crystalline iron(III) complexes have been investigated with regard to their magnetic properties. Besides ESR, Mössbauer spectroscopic investigations have also been performed.[18,19,23] In this paper, we describe the mesomorphism of iron(III) complexes containing the ligand 1,4,7-tris[3,4-bis(decyloxy)benzyl]-1,4,7-triazacyclononane (L), their thermal transformations, and the results of Mössbauer spectroscopic investigations, which revealed their octahedral structure, their bridging behavior, and a redox equilibrium of the iron centers.

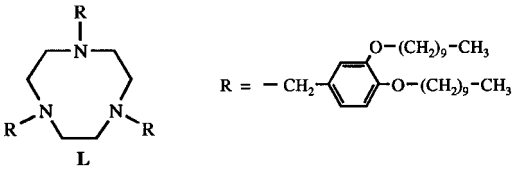

Experimental Section

Materials: Tetrahydrofuran (THF) and dioxane were dried and purified under inert gas by refluxing with potassium and subsequent distillation. Inert gas for chemical reactions (N_2 or Ar) was purified and dried in columns filled with a molecular sieve and potassium on aluminum oxide. 3,4-Bis(decyloxy)benzoyl chloride was obtained from methyl 3,4-dihydroxybenzoate (Lancaster) by a reported procedure.[29]

Instruments: FTIR: Bio Rad/Digilab FTS 40. UV/VIS: Hitachi U-3000. ^{1}H NMR: Bruker AC250 (250 MHz). GC: Waters model 510 with UV detector (Waters 440, 254 nm), RI detector (Waters 410); eluent THF; calibration with PS standards; column combination: PL-gel 600 × 7.5, pore width 100, 500 Å; particle size: 5 µm. EI/MS: Finnigan, MAT 8500; MAT 112 S Varian. Elemental analysis: Mikroanalytisches Labor Beetz Kronach; Fe: Mikroanalytisches Labor Pascher Remagen. Polarizing microscopy: Leitz Labolux 12-Pol, hot stage Mettler FP 82, Mettler FP 80; camera Wild MPS 45/51 S. DSC: Perkin-Elmer DSC 7; standard heating rate: 10 K min^{-1}. TGA: Netzsch STA 409C.

Mössbauer absorption experiments: ^{57}Co-in-Rh source at RT, standard Mössbauer cryostat; spectra were recorded between 4 K and 250 K; calculation of the spectra by least-square fits. Isomer shifts are referred to metallic iron at RT, the values for linewidth are *not* calculated in thin

[*] F. J. Litterst, G. H. Walf, R. Benda
Institut für Metallphysik, Technische Universität Braunschweig
D-38106 Braunschweig (Germany)
Fax: Int. code + 49 531 391-5129
e-mail: j.litterst@tu-bs.de
G. Lattermann, U. Stebani, S. Schmidt
Makromolekulare Chemie I, Universität Bayreuth
D-95440 Bayreuth (Germany)
Fax: Int. code + 49 921 55-3206
e-mail: guenter.lattermann@uni-bayreuth.de

  0947-6539/98/0401-0093 $ 17.50+.25/0

absorber approximation but by solving the transmission integral as described previously.[30,31] Thermal treatments were performed in a standard oven under defined atmospheric environments (air, O_2, or Ar). The Mössbauer spectra of thermally treated samples were obtained after the sample had cooled to RT, been removed from the oven, and been immediately loaded into the He atmosphere of the Mössbauer cryostat.

1,4,7-Tris[3,4-bis(decyloxy)benzyl]-1,4,7-triazacyclononane: Under inert gas, 1,4,7-triazacyclononane ([9]aneN_3, 2 mmol, Fluka), 3,4-bis(decyloxy)-benzoyl chloride (6.1 mmol), and 4-dimethylaminopyridine (DMAP) (6.1 mmol) were dissolved in dry dioxane (100 mL). The reaction mixture was stirred under reflux for 12 hours. After cooling to room temperature, DMAP·HCl was filtered off, the solvent evaporated, and the slightly yellow, oily residue purified by chromatography [alumina N, activity grade I (ICN)] with hexane/ethyl acetate 1:1, and subsequent recrystallization (methanol/THF 5:1). Yield: 50% as a white waxy solid, freeze-dried from benzene solution.

The corresponding amine ligand L was obtained by reduction of the reaction product as described earlier[6] and freeze-dried from benzene solution. The purity of the products was checked by ^{1}H NMR, IR, GPC, EI-MS, and elemental analysis.

L·$FeCl_3$[a] (Samples B and C): Anhydrous $FeCl_3$ (1.43 mmol) in dry THF (70 mL) was added dropwise at 40 °C to a solution of L (1.43 mmol) in dry THF (70 mL). The mixture was stirred at 40 °C for 12 hours, and the solvent evaporated. The residue was dissolved in hexane, insoluble particles were filtered off, and the solvent evaporated again. The residue was freeze-dried from benzene solution (sample C). Sample B was recrystallized from isooctane over a period of several weeks in the refrigerator. Yield: 96%.

Sample B: IR (KBr): $\tilde{\nu}$ = 2955, 2924, 2855, 1605, 1588, 1516, 1467, 1429, 1391, 1267, 1144, 1016 cm^{-1}; $C_{87}H_{153}Cl_3FeN_3O_6$ (1499.32 g mol^{-1}): calcd: C 69.89, H 10.28, N 2.80, Cl 7.09, Fe 3.72, O 6.40; found: a) no thermal treatment, freeze-dried: C 68.99, H 10.24, N 3.08, Cl 7.17, Fe 3.76, O 6.76; b) annealed for 30 minutes at 130 °C (H_2O atmosphere), freeze-dried: C 68.66, H 10.24, N 2.91, Cl 7.11, Fe 3.74, O 7.34; c) annealed for 2 days at 130 °C (H_2O atmosphere), freeze-dried: C 67.73, H 9.50, N 2.82, Cl 6.95, Fe 3.79, O 9.21.

L·$FeCl_3$·6H_2O[a] (Sample A): The same synthetic procedure as for [L·$FeCl_3$], but with $FeCl_3$·6H_2O. Recrystallization from diethyl ether/ethanol 1:1 over a period of several weeks in the refrigerator. Yield: 94%. IR (KBr): $\tilde{\nu}$ = 2955, 2924, 2855, 1605, 1588, 1516, 1467, 1429, 1391, 1267, 1144, 1016, 667 cm^{-1}; $C_{87}H_{153}Cl_3FeN_3O_6$ (1499.32 g mol^{-1}): calcd: C 69.89, H 10.28, N 2.80, Cl 7.09, Fe 3.72, O 6.40; found: C 69.22, H 10.36, N 3.00, Cl 6.18, Fe 3.98, O 7.26.

[a] Empirical formulae only are used here, since we do not know the precise structural formulae of the complexes.

Results

Thermal behavior: after melting at 48 °C, the two complexes of L with anhydrous $FeCl_3$ (L·$FeCl_3$, samples B and C) formed a viscous phase, M_1, which exhibited slight double refraction under the polarizing microscope (Figure 1, top). A transition to the isotropic phase was observed at 59 °C. DSC measurements of a second heat treatment (Figure 2) revealed, besides the clearing temperature, only a glass transition around 25 °C. Some small black particles still existed in the isotropic phase, but they disappeared at 130–140 °C. Surprisingly, after heating to 130–140 °C, a new mesophase was observed under the polarizing microscope on cooling to 98 °C (Figure 1, bottom). On subsequent heating, this new mesophase, M_2, exhibited a clearing temperature of 103.5 °C.

In principle, the complex of L with $FeCl_3$·6H_2O (L·$FeCl_3$·6H_2O) exhibited the same behavior with somewhat different transition temperatures. Above the melting point (47 °C), M_1 cleared at 56 °C. When heating for the first time to a maximum temperature of 140 °C (Figure 3a), DSC measurements

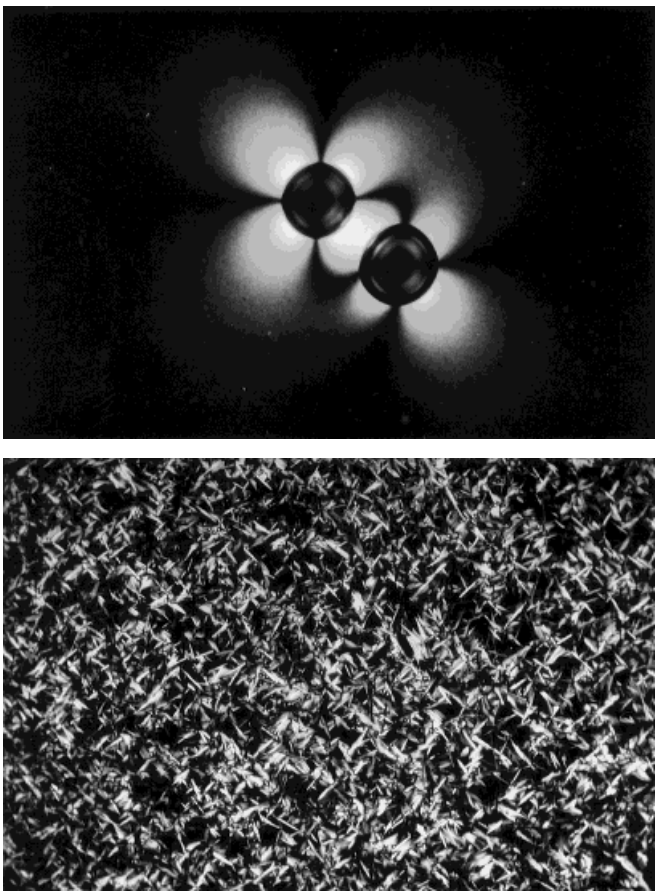

Figure 1. Optical textures of complex L·$FeCl_3$: top) M_1, at 53 °C (× 120); bottom) M_2, at 95 °C (× 120).

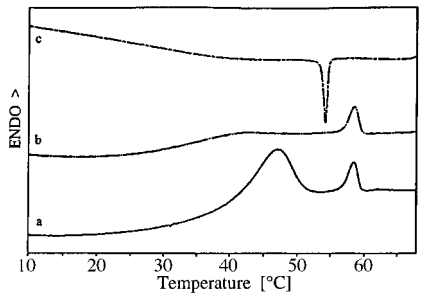

Figure 2. DSC thermogram of complex L·$FeCl_3$; T_{max} = 70 °C, heating rate: 2 K min^{-1}: a) first heating; b) second and further heatings; c) cooling.

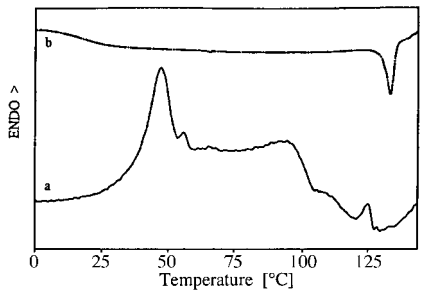

Figure 3. DSC thermogram of the complex L·$FeCl_3$·6H_2O on first heating up to 140 °C (heating rate: 10 K min^{-1}): a) first heating; b) cooling.

0947-6539/98/0401-0094 $ 17.50+.50/0 *Chem. Eur. J.* **1998**, *4*, No. 1

showed a significant change in the heat flow above 95 °C. The clearing temperature of M_2 on heating for the first time is about 125 °C. On cooling from higher temperatures in the isotropic phase (Figure 3b), M_2 reappears at 130 °C. There was no transition at ≈95 °C, no transition to M_1, and no recrystallization; however, a glass transition was detected. On further heating, besides the glass transition at 20 °C, only the clearing peak of M_2, stabilized at 136 °C, was observed. The transition temperatures of both complexes are summarized in Table 1.

Table 1. Transition temperatures, transition enthalpies (in brackets) and ΔC_p values of the complexes $L \cdot FeCl_3$ and $L \cdot FeCl_3 \cdot 6H_2O$.[a]

	T_g [°C]	ΔC_p [kJ mol^{-1} K^{-1}]	K → M_1 [°C (kJ mol^{-1})]	M_1 → M_2 [°C (kJ mol^{-1})]	M_2 → I [°C (kJ mol^{-1})]
$[L \cdot FeCl_3]$	25	0.23	53.0 (11.3)[b]	60.5 (1.1)[c]	103.5 (1.7)[d]
$[L \cdot FeCl_3 \cdot 6H_2O]$	20	0.18	47.0 (10.0)[b]	56.0 (0.8)[c]	136.0 (2.6)[d]

[a] T_g = glass transition temperature; K = crystalline phase; M = mesophase; I = isotropic phase. [b] Only on first heating. [c] Only at a maximum heating temperature of $T_{max} = 70$ °C. [d] Only on further heating, after a first maximum heating temperature of $T_{max} = 140$ °C.

The change of the heat flow around 95 °C does not correspond to the onset of the pyrolytic decomposition of the complexes at 170 °C, which was revealed by thermogravimetrical measurements (TGA). Furthermore, a dissociation (without weight loss) to the free ligand and the salt cannot explain the transition around 95 °C because of the existence of the mesophase M_2, which in consequence must then be caused by another process: a transformation of the original complex, for example. This transformation is also indicated by UV spectroscopy. In the samples not heated above 70 °C, a new band at 330 nm appeared for both complexes after annealing for 30 minutes at 130 °C.

X-ray measurements[32] of M_1 of both complexes ($L \cdot FeCl_3 \cdot 6H_2O$ and $L \cdot FeCl_3$) revealed only one reflection at 29.7 Å and a halo at 4.4 Å for the fluid alkoxy chains. This indicates the existence, but not the type, of the mesophase. In M_2, in addition to the first-order reflection at 33.7 Å and the halo at 4.4 Å, a second-order reflection at 16.9 Å was observed. This is consistent with either a columnar or a lamellar phase.

The fact that the observed transformation is not due to decomposition leads to the assumption of a modification in the coordination sphere of the complexes.

A precise determination of the complex structure by X-ray structural analysis is not possible, because of the very poor recrystallization behavior of the complexes before the thermal transformation (common for liquid crystals) and the total disappearance of the crystalline phase after the thermal transformation, even for months.

Mössbauer spectroscopy:

The initial state of the samples: In order to shed light on the situation, three samples were investigated by Mössbauer spectroscopy: Sample A corresponds to the complex $L \cdot FeCl_3 \cdot 6H_2O$, reprecipitated from a 1:1 mixture of ethanol/diethylether over a period of several weeks in the refrigerator. Both samples B and C correspond to $L \cdot FeCl_3$; sample B was reprecipitated from isooctane over a period of several weeks in the refrigerator, sample C was used directly after synthesis.

The spectra given in Figure 4 show superpositions of two quadrupole doublets (I and II) for all three samples A, B, and C, along with a further signal in the middle (IIIA, B, C). In all the samples, each of the doublets I and II exhibits the same hyperfine parameters, and the areas of the two doublets are in a ratio of 1:1. The values of the quadrupole splittings are $\Delta_I = 1.58 \pm 0.01$ and $\Delta_{II} = 1.26 \pm 0.02$ mm s^{-1}. They are nearly temperature-independent, slightly decreasing at higher temperatures ($d\Delta_{IIIA}/dT = -(2.5 \pm 0.3) \times 10^{-4}$ mm s^{-1} K^{-1}). The temperature dependence of the isomer shifts $\delta_I = 0.37 \pm 0.01$ and $\delta_{II} = 0.45 \pm 0.02$ mm s^{-1} is negligible. The parameters of linewidth for doublet I and II could be kept at the same value and the doublets' relative areas remained as 1:1 between 4 K and 200 K when fitting all the spectra (within a limit for deviation of 1%).

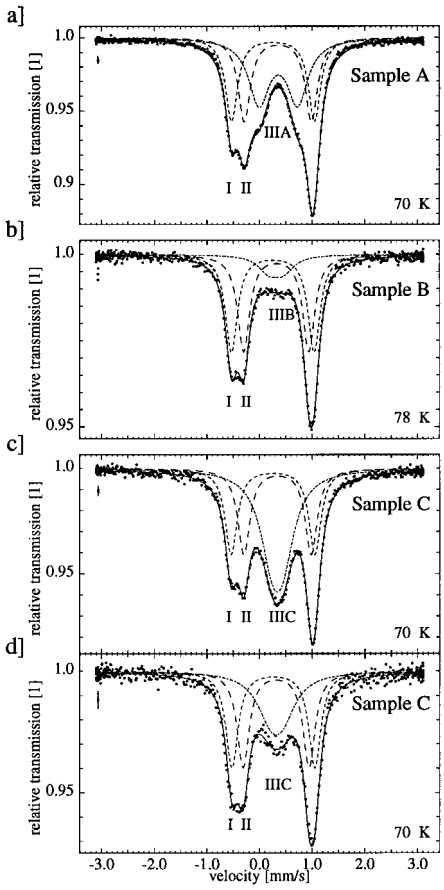

Figure 4. a–c) Mössbauer spectra of samples $L \cdot FeCl_3 \cdot 6H_2O$ (A), $L \cdot FeCl_3$ (B and C) in the initial state (i.e. without thermal treatment) at different temperatures; d) Mössbauer spectrum of sample C ($L \cdot FeCl_3$) after heating under Ar to 130 °C.

These characteristics are typical for octahedrally coordinated, binuclear *high-spin* iron(III) complexes, for example haemerythrin derivatives[33–35] as well as for nonmesogenic iron(III) complexes with 1,4,7-triazacyclononane ligands.[36,37] The two kinds of iron sites, present in a 1:1 ratio, have two slightly different environments. Therefore, this species can be regarded as an asymmetric dimer. The spectra differ in shape

and intensity with respect to the third signal in the middle. Futhermore, signal III A of sample A ($L \cdot FeCl_3 \cdot 6H_2O$) shows a broadened doublet**.** The quadrupole splitting ($\Delta_{IIIA} = 0.7 \pm 0.03\ mm\,s^{-1}$) and the weak temperature dependence of the isomer shift ($\delta_{IIIA} = 0.45 \pm 0.01\ mm\,s^{-1}$; $d\delta_{IIIA}/dT$ as for doublets I and II) are typical for monomeric *high-spin* iron(III) species.[33] At higher temperatures, the recoil-free fraction of the γ-radiation (*f*-factor) is found to decrease much more slowly than for all the other signals. Therefore, we were able to obtain spectra consisting only of the signal III A at temperatures as high as 250 K (Figure 5 c).

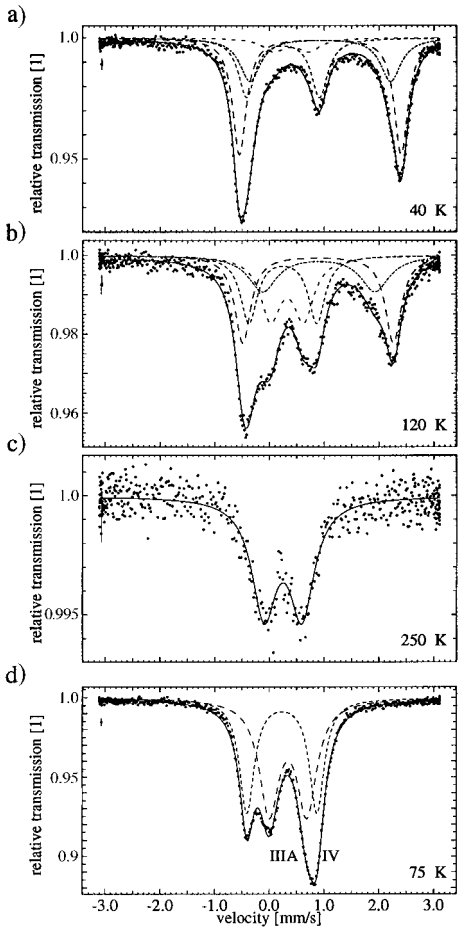

Figure 5. Mössbauer spectra of sample B $L \cdot FeCl_3$ a – c) after heating in air to 130 °C, at different temperatures; d) after storage for a few days in air at RT.

The spectra of samples B and C ($L \cdot FeCl_3$; Figure 4 b – d) show broad signals III B and III C, which are supposed to be equivalent. Because of the weakness of III B**,** we shall discuss only III C. Variation of temperature between 4 and 200 K does not change the relative area of signal III C, which is constant at all temperatures and amounts to 46 ± 2 % of the total area of all the lines added together. The fitted linewidth Γ_{IIIC} and the small quadrupole splitting Δ_{IIIC} are, however, highly correlated, which causes large uncertainties in both the parameter values (Table 2). A significant reduction of signal III C was obtained on heating this sample in an argon atmosphere. This treatment transformed equal parts of the intensity of line III C into the doublets I and II (see Figure 4 d). Therefore, III C could be interpreted as a metastable molecular modification, which is, despite a very small quadrupole splitting, closely related to the binuclear or dimeric structure corresponding to doublets I and II (asymmetric dimer), but with a high local symmetry. This interpretation as a symmetric dimer is supported by the temperature dependence of the *f*-factor, which is exactly the same for III C as for doublets I and II, but quite different from III A, which corresponds to the monomeric iron(III) structure (discussed in detail below). Apparently, the symmetrical dimer is a metastable modification first formed in the water-free complex at low temperatures and then rearranged irreversibly to the thermodynamically more stable asymmetric dimer (in the spectra seen as doublet I and II) by heating above 130 °C under an atmosphere of inert gas.

Table 2. Mössbauer hyperfine parameters. Isomer shifts are relative to metallic iron, quadrupole splittings and isomer shifts are at 70 K.

	δ [mm s^{-1}]	Δ [mm s^{-1}]	Γ [mm s^{-1}]	$B_h f$ [T]
Doublet I	0.37 ± 0.01	1.58 ± 0.01	0.151 ± 0.002	–
Doublet II	0.45 ± 0.02	1.26 ± 0.02	0.151 ± 0.002	–
IIIA	0.45 ± 0.01	0.70 ± 0.03	0.35 ± 0.05	50
IIIC	0.45 ± 0.02	$0.1 < \Delta < 0.25$	$0.3 < \Gamma < 0.5$	–
Fe(II)	1.04 ± 0.03	2.90 ± 0.01		–
Fe(II)	1.00 ± 0.06	2.40 ± 0.01		–
Doublet IV	0.37 ± 0.03	1.30 ± 0.05	0.25 ± 0.01	–

The *f*-factor is proportional to the negative exponent of the mean square displacement of the Mössbauer nucleus. In the harmonic approximation[39,40] for the atomic vibrations it is possible to derive a Debye temperature from the temperature dependence of *f*: a value of $\theta_{D,dimer} = 65$ K was determined from signals I, II, and III C, and $\theta_{D,monomer} = 86$ K from III A. We performed calculations on the *f*-factors of these two different molecular configurations, using the model of a chain of harmonic oscillators for the intramolecular oscillations and the Debye model for the intermolecular oscillations. We obtained a relative change in the Debye temperatures for monomeric molecules in comparison to dimeric ones, resulting in $\theta_{D,monomer} = \sqrt[3]{2}\,\theta_{D,dimer}$ for intermolecular oscillations (bigger molecules/longer chains have more phonon modes, i.e. they are softer) and $\theta_{D,monomer} = \sqrt{2}\,\theta_{D,dimer}$ for intramolecular oscillations (since the integrals over all Debye frequencies have to be normalized by the number of molecules, the normalization has to be done by N for bridged molecules and by $2N$ for monomer molecules), respectively. The experimental ratio of the two Debye temperatures is 0.77, which lies between the calculated values (intermolecular: 0.71, intramolecular: 0.79). This result confirms the assignment of monomeric and dimeric molecules to the related signals in the spectra.

Thermal transformations: An irreversible transformation above 130 °C was observed by DSC measurements and polarizing microscopy for samples B and C ($L \cdot FeCl_3$) under Ar. Similar behavior was found for sample A ($L \cdot FeCl_3 \cdot 6H_2O$). For a more detailed description of these transformations, we performed Mössbauer spectroscopy on all the

0947-6539/98/0401-0096 $ 17.50+.50/0 *Chem. Eur. J.* **1998**, *4*, No. 1

samples after thermal treatment in air. In principle, the results are comparable for all three samples. However, we explain the results on the basis of the spectra of sample B ($L \cdot FeCl_3$). Figure 5a–c shows a temperature scan (40–250 K) of sample B. The spectra were recorded immediately after heating to 130 °C in air and subsequent cooling to the indicated temperature. The spectrum in Figure 5d was taken after storage of the heated sample for a few days at RT in air or pure oxygen, which led to equivalent results.

The observed differences between spectra 5a–c and those obtained in the initial state prove that there has been a fundamental change of the iron environment: after heating, the initial Fe(III) compound has changed and shows at least two quadrupole doublets typical for Fe(II) ($\Delta = 2.90 \pm 0.01$ mm s^{-1}, $\delta = 1.04 \pm 0.03$ mm s^{-1} and $\Delta = 2.40 \pm 0.01$ mm s^{-1}, $\delta = 1.00 \pm 0.06$ mm s^{-1}). Their intensities become negligible for higher temperatures (Figure 5c) due to their small *f*-factor. The quadrupole splittings decrease strongly with increasing temperature; this indicates that the iron(II) centers are in the high-spin state.

The values Δ and δ of doublet IV in Figure 5d come close to those of the doublets I and II of the spectra of the same sample before thermal treatment. However, $\delta_{IV} = 0.37 \pm 0.03$ mm s^{-1} and $\Delta_{IV} = 1.30 \pm 0.05$ mm s^{-1} do not agree perfectly with either doublet I or with doublet II. The relatively high quadrupole splitting and the extremely small *f*-factor indicate a dimeric bridged structure again, but one which contains two similar iron environments that cannot be distinguished. This behavior implies that heating the samples for the first time leads to an irreversible change of the bridged iron centers from an asymmetric species with two different, well-defined iron environments to a modified bridged structure with two identical iron sites. Repeated heating of this reoxidized sample leads to the Fe(II)-dimeric configuration again, independent of the atmosphere during the heating process. This reversible Fe(II)–Fe(III) cycle has been run several times without any significant changes to either of the two different kinds of spectra (a–c and d).

The oxidation and reduction process involving binuclear molecules suggests the eventual appearance of a mixed-valent species containing a Fe(II)–Fe(III) bridge. The dynamics of charge fluctuations should show up in relaxational broadening and eventual averaging of the hyperfine interactions for fast (> GHz) fluctuations that could give more insight into the chemical process. However, our data gives no indication of the existence of such a species for the whole Fe(II)–Fe(III) cycle.

Low-temperature behavior: Some Mössbauer spectra of sample A obtained below 30 K are shown in Figure 6. A defined magnetic hyperfine pattern with six lines develops from the doublet III A. We have attributed these to the monomeric species. Similar spectra are obtained at low temperatures for samples B and C after heating in air above 130 °C.

No clear onset of the magnetic splitting can be defined, and the resonance lines are severely broadened, which points to a relaxational phenomenon with a fluctuation rate of the local magnetic field at the iron nucleus slowing down below the nuclear Larmor precession frequency. The doublet

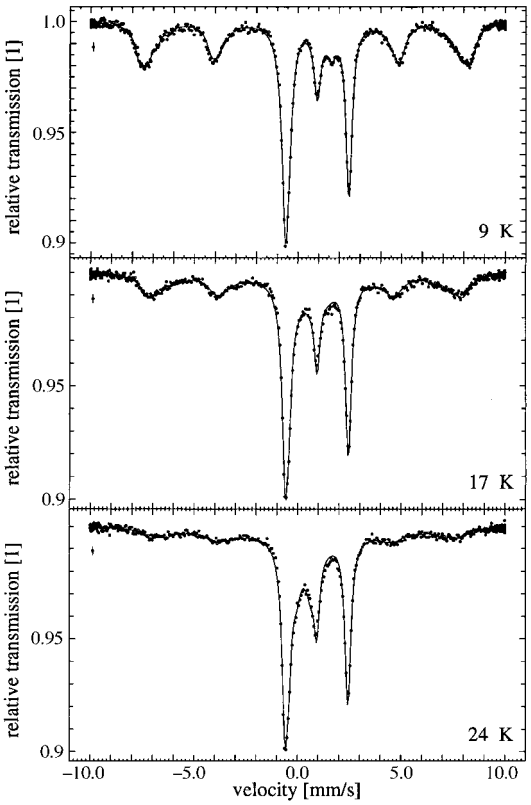

Figure 6. Mössbauer relaxation spectra at different temperatures observed for sample A $L \cdot FeCl_3 \cdot 6H_2O$ before heating to 130 °C, and for all samples after the thermal transformation in air.

signal III A transforms to the magnetic sextet, and the relative amount of the sextet increases with decreasing temperature. This indicates a wide distribution of relaxation frequencies. This is typical for a wide distribution of particle volumes and/or of magnetic anisotropies. The magnetic splitting reaches its saturation below about 9 K and corresponds to an effective magnetic hyperfine field of 50 T, which is typical for high-spin Fe(III). The angle between the main axis of the electric field gradient and the direction of the effective magnetic field can be derived by the relative line intensities of the six-line pattern and the distances between the lines 1–2 and 5–6.[33] The Mössbauer spectra reveal this angle to be 68°, which is clearly distinct from the magic angle of 55° for a random encirclement.

Even in this temperature range, the lines are still broadened, which indicates a considerable inhomogeneous static distribution of the magnetic hyperfine interaction.

Similar relaxational spectra are usual for small particles of different iron oxides or hydroxides whose magnetizations become blocked at low temperatures. Such particles could have precipitated in our samples as decomposition products. There are, however, arguments against this interpretation. Firstly, the recoil-free fraction of the observed signal is very low: for oxide precipitates one would expect a strong absorption signal to persist above room temperature, which is not the case here. Secondly, the relative amount of signal III A with respect to the total spectral area increases upon slower cooling and decreases for fast quenching. These

reversible changes are not expected for a decomposition product; rather, they reflect the kinetics of the monomer formation.

Slow paramagnetic relaxation of isolated Fe^{3+} as the origin of the relaxation spectra can be excluded, since the splitting of Kramer's doublets for an *S*-state ion is very small compared to the thermal energies. We thus propose that the magnetic hyperfine patterns arise from magnetic ordering between the monomeric species. This means that the monomeric molecules form regular structures that enable the iron centers to couple magnetically through exchange interactions and to establish a static magnetic order at low temperatures (<40 K). This magnetic order becomes possible only for the expected regular stacking of the monomeric molecules, which brings the magnetic ions into close proximity. Both the dynamic and the static broadenings observed result from short-range order connected with structural disorder, but also with the low-dimensional character of the magnetic coupling. A thorough investigation of the magnetic properties and their dependence on the molecular structure is in progress.

Discussion and Conclusions

Mössbauer spectroscopic measurements demonstrate that the peculiar thermal behavior of the liquid crystalline iron(III) complexes with the 1,4,7-tris[3,4-bis(decyloxy)benzyl]-1,4,7-triazacyclononane ligand, L, is due to the existence of various monomeric and dimeric species as well as reversible redox reactions. The results are summarized in Scheme 1.

The presence of water or oxygen is of crucial importance for the formation of the monomeric iron(III) species as well as for the redox reaction. Under inert gas in anhydrous conditions, samples B and C ($L\cdot FeCl_3$) do not form the monomeric iron(III) species (see Figure 5d). In the presence of water, the monomeric species is formed directly in sample A ($L\cdot FeCl_3\cdot 6H_2O$; see Figure 5a). In samples B and C it is formed after thermal treatment or even if kept in air (Figure 5d).

On the other hand, the reduction of Fe(III) to Fe(II) occurs on heating A, B, or C above 130 °C; for A ($L\cdot FeCl_3\cdot 6H_2O$) the reduction occurs even under argon. Therefore, the reduction process seems to be connected with the presence of water—air humidity in the case of B and C, crystal water in the case of A. It is possible that the process depends on the formation of aquo or hydroxo ligands (doublet IV), which would have replaced chloro ligands. A further hydrolysis product could then be the monomeric iron(III) species. Another indication for the role of water in a hydrolysis and reduction process is the observation that the thermal transformation around 130 °C apparently occurred much faster for $L\cdot FeCl_3\cdot 6H_2O$, which allows the detection of the transformation in DSC measurements (see Figure 3). Finally, annealing the water-free sample $L\cdot FeCl_3$ (B, C) in water vapor at 130 °C for 30 min (annealing in air for 2 days gives the same results) increased the oxygen content and decreased the chlorine content in the sample, as shown by elemental analysis, which demonstrates the suggested replacement of chloro ligands.

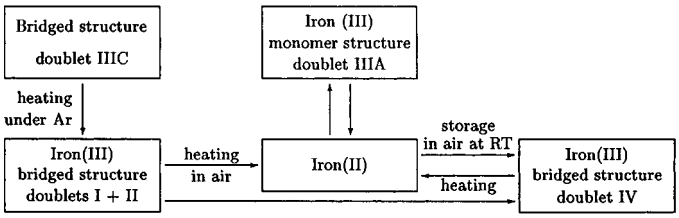

Scheme 1. Reaction scheme of iron(III) complexes with the 3,4-bis(decyloxy)benzyl-substituted 1,4,7-triazacyclononane ligand L deduced from Mössbauer spectroscopy.

From these facts we propose a possible reaction scheme in terms of molecular structures (Scheme 2). A pentacoordinated iron(III) center (belonging here to the asymmetric dimer) has also been postulated in binuclear haemerythrin iron complexes.[35] The existence of μ-hydroxo or μ-oxo bridges has been reported in complexes with a 1,4,7-triazacyclononane derivative core.[36–38,41] Additionally, responsibility for the formation of oxo bridges in a liquid crystalline, ferrocene-containing Schiff base has been ascribed to atmospheric moisture.[42] With respect to the redox process, a similar mechanism involving oxygen and H_2O was established for the interconversion of various forms of haemerythrin.[42]

With respect to liquid crystallinity, the investigations presented here lead to the conclusion that the low-temperature mesophase, M_1, is related to the asymmetric dimer. The high-temperature mesophase, M_2, formed after the thermal treatment at 130 °C must then result either from the monomer or the dimeric compound formed by the hydrolysis process.

Analogous or similar complexes of iron(III)chloride with [9]aneN_3 derivatives have always been reported as monomeric.[36–38] Bridged binuclear complexes have only been obtained by subsequent specific reactions.[36–38,41] To our knowledge, a thermally induced redox equilibrium has never been described. Only an air oxidation of a binuclear iron(II)

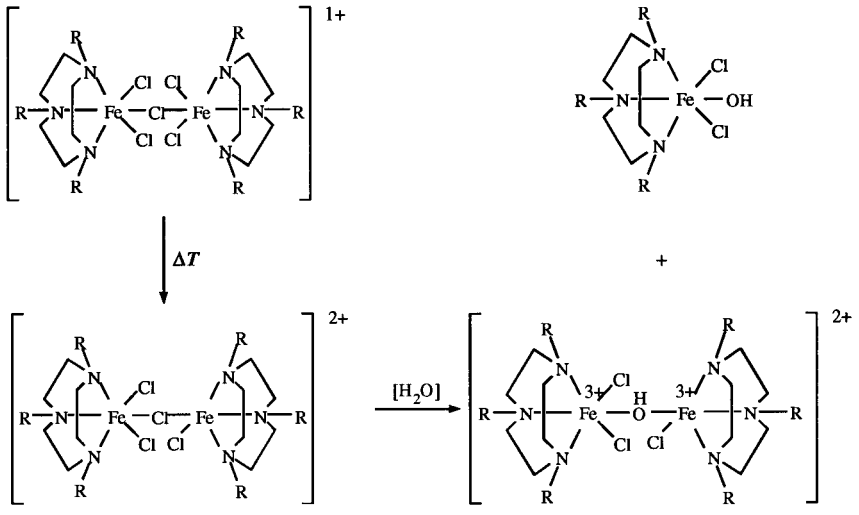

Scheme 2. Possible reaction scheme for hydrolysis of iron(III) complexes with ligand L.

0947-6539/98/0401-0098 $ 17.50+.50/0 *Chem. Eur. J.* **1998**, *4*, No. 1

complex with a substituted [9]aneN_3 ligand to a stable iron(III) product has been observed.[36] On the other hand, redox processes involving metal complexes of 1,4,7-substituted [9]aneN_3 ligands are described for binuclear complexes with manganese,[43] which can be used in detergent additives as very efficient catalysts for low-temperature bleaching processes.[44,45]

It is obviously significant that the described behavior of the presented iron complexes is closely related to the presence of ligand L. At the present, we do not know whether it is only the steric situation of the bulky substituents, the influence of long alkyl side chains on transition temperatures, or the liquid crystalline state, with its additional degree of order, which is responsible for the described bridging and redox reactions of this example of metallomesogen.

Acknowledgments: U.S., S.S., and G.L. gratefully acknowledge the financial support of the Deutsche Forschungsgemeinschaft (DFG La 662/1–2).

Received: April 29, 1997 [F682]

[1] A.-M. Giroud-Godquin, P. M. Maitlis, *Angew. Chem.* **1991**, *103*, 370, *Angew. Chem. Int.Ed. Engl*. **1991**, *30*, 375.
[2] P. Espinet, M. A. Esteruelas, L. A. Oro, J. L. Serrano, E. Sola, *Coord. Chem. Rev.* **1992**, *117*, 215.
[3] S. A. Hudson, P. M. Maitlis, *Chem. Rev.* **1992**, 93, 861.
[4] L. Oriol, J. L. Serrano, *Adv. Mater.* **1995**, ***7***, 348.
[5] *Metallomesogens* (Ed.: J. L. Serrano), VCH, Weinheim, **1996**.
[6] G. Lattermann, S. Schmidt, R. Kleppinger, J. H. Wendorff, *Adv. Mater.* **1992**, *4,* 30.
[7] S. Schmidt, G. Lattermann, R. Kleppinger, J. H. Wendorff, *Liq. Cryst.* **1994**, *16*, 693.
[8] H. Zheng, T. M. Swager, *J. Am. Chem. Soc*. **1994**, *116*, 761.
[9] D. W. Bruce, *Adv. Mater*. **1994**, *6*, 699.
[10] D. W. Bruce, X.-H. Liu, *J. Chem. Soc. Chem. Commun.* **1994**, 729.
[11] S. Morrone, G. Harrison, D. W. Bruce, *Adv. Mater.* **1995**, *7*, 665.
[12] D. W. Bruce, X.-H. Liu, *Liq. Cryst.* **1995**, *18*, 165.
[13] T. M. Swager, H. Zeng, *Mol. Cryst. Liq. Cryst.* **1995**, *260***,** 301.
[14] U. Stebani, G. Lattermann, M. Wittenberg, J. H. Wendorff, *Angew. Chem. Int. Ed. Engl*. **1996**, *35*, 1858.
[15] Y. G. Galyametdinov, G. I. Ivanova, I. V. Ovchinikov, *Izv. Akad. Nauk. SSSR Ser. Khim.* **1989**, 1931.
[16] L. Ziminski, J. Malthête, *J. Chem. Soc. Chem. Commun.* **1990**, 1495.
[17] P. Jacq, J. Malthête, *Liq. Cryst.* **1996**, *21*, 291.
[18] V. G. Bekeshev, V. Y. Rochev, E. F. Makarov, *Mol. Cryst. Liq. Cryst.* **1990**, *192*, 131.
[19] V. G. Bekeshev, V. Y. Rochev, E. F. Makarov, *Hyperfine Interact.* **1991**, *67*, 661.
[20] Y. Galyametdinov, G. Ivanova, K. Griesar, A. Prosvirin, I. Ovchinikov, W. Haase, *Adv. Mater.* **1992**, *4*, 739.
[21] W. Haase, K. Griesar, M. F. Iskander, Y. Galyametdinov, *Mol. Cryst. Liq. Cryst.* **1993**, *3*, 115.
[22] D. Huang, J. Yang, L. Zhang, Y. Liu, S. Xiang, *Hecheng Huaxue* **1994,** *2*, 1.
[23] N. E. Domracheva, Y. G. Galyametdinov, R. A. Manapov, A. V. Prosvirin, I. V. Ovchinnikov, W. Haase, K. Griesar, *Fiz. Tverd. Tela (St. Petersburg)* **1994**, *36*, 2154.
[24] Y. G. Galyametdinov, O. N. Kadkin, A. V. Prosvirin, *Izv. Akad. Nauk. Ser. Khim.* **1994**, 941.
[25] M. Marcos, J. L. Serrano, P. J. Alonso, J. I. Martinez, *Adv. Mater.* **1995**, *7*, 173.
[26] K. Hanabusa, J. Higashi, T. Koyama, H. Shirai, N. Hojo, A. Kurose, *Makromol. Chem.* **1989***, 190*, 1.
[27] P. Singh, M. D. Rausch, R. W. Lenz, *Polymer Bull.* **1989***, 22*, 247.
[28] P. J. Alonso, J. I. Martinez, L. Oriol, M. Pinol, J. L. Serrano, *Adv. Mater.* **1994**, *6*, 663.
[29] G. Staufer, G. Lattermann, *Makromol. Chem.* **1991**, *192*, 2421.
[30] W. Stieler, M. Hillberg, F. J. Litterst, C. Böttger, J. Hesse, *Nucl. Instrum. Methods Phys. Res. Sect. B* **1995**, 235.
[31] W. Wagener, M. Hillberg, R. Feyerherm, W. Stieler, F. J. Litterst, T. Pöhlmann, O. Nuyken, *J. Phys.: Condens. Matter* **1994**, *6*, L391.
[32] M. Wittenberg, J. H. Wendorff, Marburg, personal communication.
[33] N. N. Greenwood, T. C. Gibb, *Mössbauer Spectroscopy*, Chapman & Hall Ltd., London, **1971**.
[34] K. S. Murray, *Coord. Chem. Rev.* **1974**, *12*, 1.
[35] R. G. Wilkins, *Chem. Soc. Rev.* **1992**, 171.
[36] J. R. Hartmann, R. L. Rardin, P. Chaudhuri, K. Pohl, K. Wieghardt, B. Nuber, J. Weiss, G. C. Papaefthymiou, R. B. Frankel, S. J. Lippard, J. *Am. Chem. Soc.* **1987***, 109*, 7387.
[37] R. Hotzelmann, K. Wieghardt, U. Flörke, H.-J. Haupt, *Angew. Chem.* **1990**, *102*, 720; *Angew. Chem. Int. Ed. Engl.* **1990**, *129*, 645.
[38] C. Flassbeck, K. Wieghardt, *Z. Anorg. Allg. Chem*. **1992**, *608*, 60.
[39] J. G. Dash, D. P. Johnson, W. M. Visscher, *Phys. Rev.* **1968**, *168*, 1087.
[40] R. M. Housley, F. Hess, *Phys. Rev*. **1966**, *146*, 517.
[41] K. Wieghardt, S. Drüecke, P. Chaudhuri, *Z. Naturforsch. B* **1989**, *44*, 1093.
[42] Y. G. Galyametdinov, O. N. Kadkin, A. V. Prosvirin, *Russ. Chem. Bull.* **1994**, *43*, 887.
[43] U. Bossek, T. Weyermüller, K. Wieghardt, B. Nuber, J. Weiss, *J. Am. Chem. Soc.* **1990**, *112*, 6387.
[44] A. E. Comyns, *Nature*, **1994**, *369*, 609.
[45] R. Hage, J. E. Iburg, J. Kerschner, J. H. Koek, E. L. M. Lempers, R. J. Martens, U. S. Racherla, S. W. Russel, T. Swarthoff, M. R. P. van Vliet, J. B. Warnaar, L. van der Wolf, B. Krijnen, *Nature*, **1994**, *329*, 637.